Ionization of deep Te donor in Te-doped $Al_{0.6}Ga_{0.4}Sb$ epilayers

Hideharu Matsuura[a] and Kazuhiro Nishikawa
Department of Electronic Engineering and Computer Science, Osaka Electro-Communication University, 18-8 Hatsu-cho, Neyagawa, Osaka 572-8530, Japan

(Received 7 December 2004; accepted 18 February 2005; published online 20 April 2005)

The temperature dependence of the electron concentration $n(T)$ for a Te-doped $Al_xGa_{1-x}Sb$ epilayer with $x=0.2$ or $x=0.6$ is obtained from Hall-effect measurements. The density N_D and energy level ΔE_D of Te donors are determined by the graphical peak analysis method (i.e., free-carrier concentration spectroscopy) from the $n(T)$. Since the donor level of Te is shallow in $Al_{0.2}Ga_{0.8}Sb$, the Fermi–Dirac distribution function, which does not include the influence of the excited states of the Te donors, can be applied to determining N_D and ΔE_D. In $Al_{0.6}Ga_{0.4}Sb$, on the other hand, a proposed distribution function including this influence is elucidated to be necessary to the determination of N_D and ΔE_D, because Te acts as a deep donor. Moreover, the excited states of the Te donors in $Al_{0.6}Ga_{0.4}Sb$ are found to enhance the ionization efficiency of the Te donors at elevated temperatures. © *2005 American Institute of Physics*. [DOI: 10.1063/1.1887832]

I. INTRODUCTION

GaSb-based semiconductors have been regarded as a promising semiconductor for near- and midinfrared laser diodes and photodiodes, which can be used for monitoring the concentrations of CO_2, CO, NO_x, and SO_x in the atmosphere.[1] In order to fabricate a device-quality *n*-type or *p*-type GaSb-based epilayer, it is necessary to lower the densities of electrically active residual impurities and defects in undoped GaSb-based epilayers before dopants (i.e., donors or acceptors) are put into them. Next, investigating a dopant with low ionization energy is necessary to a good-quality *n*-type or *p*-type epilayer. This is why an accurate determination of the densities and energy levels of acceptors or donors in undoped and doped GaSb-based epilayers is essential.

In GaSb-based laser diodes, *n*-type or *p*-type $Al_xGa_{1-x}Sb$ epilayers, which have a band gap wider than well layers (e.g., $In_xGa_{1-x}Sb$) acting as an active layer, play an important role in injecting electrons or holes into the well layers. According to the literature,[2,3] $Al_xGa_{1-x}Sb$ changes from a direct band-gap semiconductor to an indirect band-gap semiconductor when the Al mole fraction (x) increases, suggesting that the change of the band structure must affect the ionization energy (i.e., donor level) of donors. For example, the donor level of Te or Si was reported to be deep at $x>0.2$ in $Al_xGa_{1-x}As$,[4,5] and also the Si donor level was deep in GaAs under pressure.[6] Therefore, it is necessary to investigate the dependence of the Te donor level in Te-doped $Al_xGa_{1-x}Sb$ epilayers on x, while Te acts as a shallow donor in GaSb.[7]

Deep level transient spectroscopy[8] is a powerful method for investigating deep level defects and impurities. In order to accurately determine the densities and energy levels of them, however, their densities should be much less than the dopant density.[9]

In order to study the energy levels and densities of dopants, Hall-effect measurements are usually conducted. Although the donor levels and donor densities are determined using the temperature dependence of the electron concentration $n(T)$, there are the following problems in the analyses of the $n(T)$. In semiconductors with more than one donor species or in compensated semiconductors, the actual donor levels cannot be determined from the slopes of the $n(T)-1/T$ plot.[10,11] Moreover, it is difficult to obtain reliable results by fitting a curve to the experimental $n(T)$, because too many curve-fitting parameters (i.e., the densities and energy levels of several donor species) must be simultaneously determined. In order to reduce the number of the curve-fitting parameters, some assumptions regarding the donor species are usually adopted.

Without any assumptions regarding the donor species, graphical peak analysis methods can uniquely determine the densities and energy levels of donors. As a powerful graphical peak analysis method, free-carrier concentration spectroscopy (FCCS) has been proposed and tested.[10–19]

When the dopant level is deep, it is reported that the excited states of the dopant strongly influence the majority-carrier concentration.[20–26] For example, in Al-doped *p*-type SiC or Mg-doped *p*-type GaN, the acceptor density and acceptor level are usually determined by a least squares fit of the charge neutrality equation to the temperature dependence of the hole concentration $p(T)$ using the Fermi–Dirac distribution function, which does not include the influence of the excited states of acceptors. The determined acceptor level is deep in Al-doped SiC or Mg-doped GaN, which is consistent with the acceptor level determined from photoluminescence studies.[27,28] On the other hand, the determined acceptor density is always much higher than the concentration of Al or Mg atoms determined by secondary-ion-mass spectroscopy,[20–26,29–33] indicating that a distribution function suitable for these deep acceptors is necessary to the analysis of the $p(T)$. Recently, the distribution function including the influence of the excited states of deep dopants has been proposed and tested.[20–26]

In this paper, we report on our investigation of the energy level and density of Te donors in Te-doped $Al_xGa_{1-x}Sb$

[a]Electronic-mail: matsuura@isc.osakac.ac.jp

epilayers with $x=0.2$ or $x=0.6$. In order to determine the donor level and density from the $n(T)$ obtained by the Hall–effect measurement, we apply the FCCS that can determine them using any distribution function (e.g., the Fermi–Dirac distribution function or the proposed distribution function including the influence of the excited states of donors).

II. DISTRIBUTION FUNCTION FOR DEEP DONORS

A. The number of configurations of the system

Electrons in semiconductors are fermions, which obey the Pauli exclusion principle. As a consequence, in the allowed bands, the multiplicity function $W_B(E_i)$ for the $n_e(E_i)$ electrons arranged in the $D(E_i)$ states at a given energy E_i is expressed as[34]

$$W_B(E_i) = \frac{D(E_i)!}{[D(E_i) - n_e(E_i)]!n_e(E_i)!}, \tag{1}$$

where $D(E_i)$ is the number of degenerate states at E_i per unit volume and $n_e(E_i)$ is the number of electrons at E_i per unit volume.

In a forbidden band, on the other hand, the multiplicity function for the n_D electrons arranged in the N_D donors is quite different from Eq. (1), where N_D is the number of donors per unit volume and n_D is the number of electrons bound to donors per unit volume. When spin degeneracy as well as the excited states of the donor is neglected, the multiplicity function W_{D1} for the n_D electrons arranged in the N_D donors is given by

$$W_{D1} = \frac{N_D!}{(N_D - n_D)!n_D!}. \tag{2}$$

Each state of the ground state and the excited states consists of a spin-up state and a spin-down state. When the difference in energy between the two states under a magnetic field is denoted by ΔE_{spin}, the partition function for one electron arranged in the two states is expressed as

$$1 + \exp\left(-\frac{\Delta E_{\text{spin}}}{kT}\right). \tag{3}$$

For the n_D electrons, therefore, the multiplicity function W_{D2} is given by

$$W_{D2} = \left[1 + \exp\left(-\frac{\Delta E_{\text{spin}}}{kT}\right)\right]^{n_D}. \tag{4}$$

When the magnetic field is not or weakly applied to the semiconductor ($\Delta E_{\text{spin}} \cong 0$),

$$W_{D2} \cong 2^{n_D}. \tag{5}$$

In a neutral donor, furthermore, only an excess electron is bound to one state of the ground state and the excited states of the donor. The partition function for one electron arranged in them is expressed as

$$g_1 + \sum_{r=2}^{l} g_r \exp\left(-\frac{E_r - E_D}{kT}\right), \tag{6}$$

where E_r is the $(r-1)$th excited-state level ($r \geqslant 2$), g_1 is the ground-state degeneracy factor of 1, g_r is the $(r-1)$th excited-state degeneracy factor of r^2,[35,36] $l-1$ is the highest order of the excited states considered here, and k is the Boltzmann constant. For the n_D electrons, therefore, the multiplicity function W_{D3} is given by

$$W_{D3} = \left[g_1 + \sum_{r=2}^{l} g_r \exp\left(-\frac{E_r - E_D}{kT}\right)\right]^{n_D}. \tag{7}$$

Consequently, the multiplicity function W_D for the n_D electrons arranged in the N_D donors is expressed as

$$W_D = W_{D1}W_{D2}W_{D3}. \tag{8}$$

Finally, the total number W of configurations of the system is obtained from the product of these multiplicities as

$$W = W_D \prod_i W_{Bi}. \tag{9}$$

B. Thermal equilibrium configuration

The thermal equilibrium configuration occurs when the entropy

$$S = k \ln W \tag{10}$$

becomes a maximum value under the following two conservation laws: (1) the total number n_{total} of electrons in the system is conserved, that is,

$$n_{\text{total}} = n_D + \sum_i n(E_i) = \text{const} \tag{11}$$

and (2) the total energy E_{total} of electrons in the system is conserved, i.e.,

$$E_{\text{total}} = \overline{E_D(T)}n_D + \sum_i E_i n(E_i) = \text{const}, \tag{12}$$

where $\overline{E_D(T)}$ is the average donor level and $\overline{E_{\text{exl}}(T)}$ is the ensemble average of the ground- and excited-state levels of the donor. Under these conditions, the distribution functions for electrons can be derived.[20] In the following, all the energy levels are measured from E_C (i.e., $\Delta E = E_C - E$).

The distribution function including the influence of the excited states of donors is derived as

$$f_l(\Delta E_D) = \frac{1}{1 + \dfrac{1}{g_{Dl}(T)} \exp\left[\dfrac{\Delta E_F(T) - \Delta E_D}{kT}\right]}, \tag{13}$$

where $\Delta E_F(T)$ is the Fermi level at T and $g_{Dl}(T)$ is the effective donor degeneracy factor given by

$$g_{Dl}(T) = 2\left[1 + \sum_{r=2}^{l} g_r \exp\left(-\frac{\Delta E_D - \Delta E_r}{kT}\right)\right] \times \exp\left[-\frac{\overline{E_{\text{exl}}(T)}}{kT}\right], \tag{14}$$

$$\overline{E_{exl}(T)} = \frac{\sum_{r=2}^{l} (\Delta E_D - \Delta E_r) g_r \exp\left(-\frac{\Delta E_D - \Delta E_r}{kT}\right)}{1 + \sum_{r=2}^{l} g_r \exp\left(-\frac{\Delta E_D - \Delta E_r}{kT}\right)}, \quad (15)$$

and

$$\overline{\Delta E_D(T)} = \Delta E_D - \overline{E_{exl}(T)}. \quad (16)$$

When the influence of the excited states is ignored [i.e., $l=1$ and $\overline{E_{exl}(T)}=0$], Eq. (13) coincides with the Fermi–Dirac distribution function for donors;

$$f_{FD}(\Delta E_D) = \frac{1}{1 + \frac{1}{2}\exp\left[\frac{\Delta E_F(T) - \Delta E_D}{kT}\right]}. \quad (17)$$

C. The hydrogenic donor case

A neutral donor can be approximately described as a hydrogen atom, that is, a positively charged ionized donor and an electron in orbit about the donor. In this case, the ΔE_r is given by[37,38]

$$\Delta E_r = \frac{q^4 m_n^*}{8h^2 \epsilon_s^2 \epsilon_0^2 r^2} = 13.6 \frac{m_n^*}{m_0} \frac{1}{\epsilon_s^2} \frac{1}{r^2} (\text{eV}), \quad (18)$$

where q is the electron charge, m_n^* is the electron effective mass in the semiconductor, m_0 is the free-space electron mass, h is the Planck's constant, ϵ_s is the semiconductor dielectric constant, and ϵ_0 is the free-space permittivity.

On the other hand, the ΔE_D is expressed as

$$\Delta E_D = \Delta E_1 + E_{CCC}, \quad (19)$$

where E_{CCC} is the central-cell correction induced due to a strongly localized potential such as a strain field around the donor.[39]

III. FREE-CARRIER CONCENTRATION SPECTROSCOPY

In the following, we assume an n-type semiconductor with n types of donor species (N_{Di}: the ith donor density, ΔE_{Di}: the ith donor level) and a total acceptor density ($N_{A,\text{total}}$). From the charge neutrality condition, the $n(T)$ can be expressed as[40]

$$n(T) = \sum_{i=1}^{n} N_{Di}[1 - F(\Delta E_{Di})] - N_{A,\text{total}} \quad (20)$$

in the temperature range in which $p(T)$ is much less than $n(T)$. Here, $F(\Delta E_{Di})$ is either distribution function for donors $f_{FD}(\Delta E_{Di})$ or $f_l(\Delta E_{Di})$. Using the effective density of states $N_C(T)$ in the conduction band, on the other hand, the $n(T)$ is given by[40]

$$n(T) = N_C(T) \exp\left[-\frac{\Delta E_F(T)}{kT}\right], \quad (21)$$

where

$$N_C(T) = N_{C0} k^{3/2} T^{3/2}, \quad (22)$$

$$N_{C0} = 2\left(\frac{2\pi m_n^*}{h^2}\right)^{3/2} M_C, \quad (23)$$

and M_C is the number of equivalent minima in the conduction band.

From Eqs. (20) and (21), a favorable function to determine N_{Di} and ΔE_{Di} can be introduced as follows. The function to be evaluated is defined as[14–26]

$$H(T, E_{\text{ref}}) \equiv \frac{n(T)^2}{(kT)^{5/2}} \exp\left(\frac{E_{\text{ref}}}{kT}\right), \quad (24)$$

where E_{ref} is the parameter which can shift the peak temperature of $H(T, E_{\text{ref}})$ within the measurement temperature range. Substituting Eq. (20) for one of the $n(T)$ in Eq. (24) and substituting Eq. (21) for the other $n(T)$ in Eq. (24) yield

$$H(T, E_{\text{ref}}) = \sum_{i=1}^{n} \frac{N_{Di}}{kT} \exp\left(-\frac{\Delta E_{Di} - E_{\text{ref}}}{kT}\right) I(\Delta E_{Di}) - \frac{N_{A,\text{total}} N_{C0}}{kT} \exp\left[\frac{E_{\text{ref}} - \Delta E_F(T)}{kT}\right], \quad (25)$$

where

$$I(\Delta E_{Di}) = N_{C0} \exp\left[\frac{\Delta E_{Di} - \Delta E_F(T)}{kT}\right] F(\Delta E_{Di}). \quad (26)$$

The function

$$\frac{N_{Di}}{kT} \exp\left(-\frac{\Delta E_{Di} - E_{\text{ref}}}{kT}\right) \quad (27)$$

in Eq. (25) has a peak value of $N_{Di}\exp(-1)/kT_{\text{peak}i}$ at the peak temperature,

$$T_{\text{peak } i} = \frac{\Delta E_{Di} - E_{\text{ref}}}{k}. \quad (28)$$

As is clear from Eq. (28), the E_{ref} can shift the peak of $H(T, E_{\text{ref}})$ within the temperature range of the measurement. Although the actual $T_{\text{peak}i}$ of $H(T, E_{\text{ref}})$ is slightly different from the $T_{\text{peak}i}$ calculated by Eq. (28) due to the temperature dependence of $I(\Delta E_{Di})$, we can easily determine the accurate values of N_{Di} and ΔE_{Di} from the peak of the experimental $H(T, E_{\text{ref}})$, using a personal computer. The WINDOWS application software for the FCCS can be freely downloaded at our web site (http://www.osakac.ac.jp/labs/matsuura/). This software can also evaluate them by using the curve-fitting method.

IV. EXPERIMENT

Four 2-μm-thick epilayers (undoped $Al_{0.6}Ga_{0.4}Sb$, two Te-doped $Al_{0.6}Ga_{0.4}Sb$ with different Te-doping densities, and Te-doped $Al_{0.2}Ga_{0.8}Sb$) were grown on semi-insulating GaAs(100) substrates at 470 °C by water-cooled molecular-beam epitaxy. The temperature of the Knudsen cell for Ga was 910 °C, and the temperature of the crystal cell for Sb_4 was 460 °C. The $Al_{0.2}Ga_{0.8}Sb$ epilayer was grown at the temperature (T_{Al}) of the Knudsen cell for Al of 1010 °C, while the $Al_{0.6}Ga_{0.4}Sb$ epilayers were grown at T_{Al} = 1084 °C. The mole fractions of Al were determined using

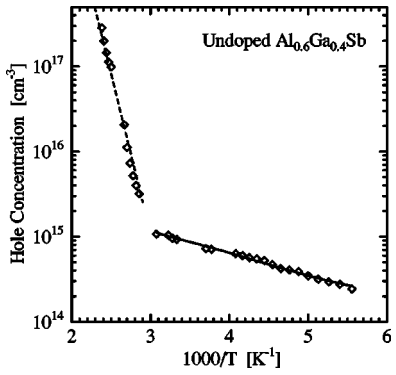

FIG. 1. Temperature dependence of hole concentration in undoped $Al_{0.6}Ga_{0.4}Sb$ epilayer.

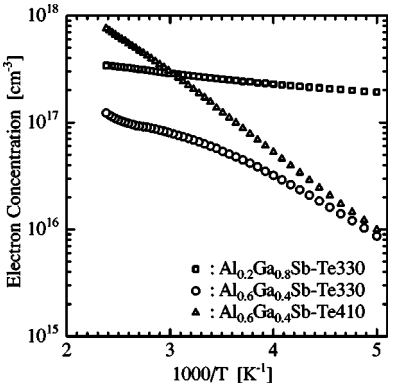

FIG. 2. Temperature dependence of electron concentration.

x-ray diffraction. In order to put Te into the epilayers, the temperature (T_{Te}) of the Knudsen cell for Ga_2Te_3 was 330 or 410 °C. The following four samples were measured: undoped $Al_{0.6}Ga_{0.4}Sb$, Te-doped $Al_{0.6}Ga_{0.4}Sb$ with $T_{\mathrm{Te}}=330$ °C ($Al_{0.6}Ga_{0.4}Sb-Te330$), Te-doped $Al_{0.6}Ga_{0.4}Sb$ with $T_{\mathrm{Te}}=410$ °C ($Al_{0.6}Ga_{0.4}Sb-Te410$), and Te-doped $Al_{0.6}Ga_{0.4}Sb$ with $T_{\mathrm{Te}}=330$ °C ($Al_{0.2}Ga_{0.4}Sb-Te330$). After each epilayer was cut into a 7×7-mm^2 size, the Hall-effect measurements were carried out in the van der Pauw configuration in a magnetic field of 1.4 T and at a current of 0.1 mA using a modified MMR Technologies' Hall system.

V. RESULTS AND DISCUSSION

The diamonds in Fig. 1 represent the experimental $p(T)$ for the undoped $Al_{0.6}Ga_{0.4}Sb$ epilayer that exhibits p-type conduction. At high temperatures ($1000/T<3$), this epilayer exhibits intrinsic behavior. From the steep slope (broken straight line) in Fig. 1, the band gap E_g of this epilayer is determined as ~1.5 eV, which is between $E_g=0.75$ eV for GaSb and $E_g=1.61$ eV for AlSb.[41] At low temperatures ($1000/T>3$), the $p(T)$ is strongly affected by residual acceptors (i.e., impurities and defects). The FCCS signal has two peaks, indicating that at least two types of acceptor species are included in this epilayer. From each peak, the energy level ΔE_{Ai} and density N_{Ai} of the corresponding acceptor are determined. The determined values of ΔE_{A2} and N_{A2} are 117 meV and 1.96×10^{14} cm^{-3}, while ΔE_{A3} and N_{A3} are determined as 167 meV and 9.22×10^{14} cm^{-3}. Moreover, this epilayer is found to include the shallow acceptors completely ionized below the lowest measurement temperature. The value of $N_{A1}-N_{D,\mathrm{total}}$ is estimated as 1.13×10^{14} cm^{-3}, where N_{A1} is the density of the shallow acceptors and $N_{D,\mathrm{total}}$ is the total donor density. The solid curve represents the $p(T)$ simulation using Eqs. (20) and (21) with the determined values. The values of ΔE_{A2} and ΔE_{A3} are close to those reported in undoped GaSb epilayers.[16] From this result, it is found that the residual acceptor density in our $Al_{0.6}Ga_{0.4}Sb$ epilayers is $\sim10^{15}$ cm^{-3}.

Figure 2 shows $n(T)$ for $Al_{0.2}Ga_{0.8}Sb-Te330$ (squares), $Al_{0.6}Ga_{0.2}Sb-Te330$ (circles), and $Al_{0.6}Ga_{0.4}Sb-Te410$ (triangles). $Al_{0.2}Ga_{0.8}Sb$ is expected to be a direct band-gap semiconductor similar to GaSb, while $Al_{0.6}Ga_{0.4}Sb$ is an indirect band-gap semiconductor similar to AlSb whose conduction minima are located near X.[2,3] Judging from the slope of $n(T)-1/T$ for $Al_{0.2}Ga_{0.8}Sb-Te330$, the substitutional Te donors in $Al_{0.2}Ga_{0.8}Sb$ act as a shallow donor. On the other hand, since the slopes of $n(T)-1/T$ for $Al_{0.6}Ga_{0.4}Sb$ are steeper, the substitutional Te donors in $Al_{0.6}Ga_{0.4}Sb$ are considered to act as a deep donor, which is similar to Si donors or Te donors in $Al_xGa_{1-x}As$ with $x>0.2$.[4,5] By comparison with Fig. 1, the intrinsic behavior appears at high temperatures ($1000/T<2.5$) in $Al_{0.6}Ga_{0.2}Sb-Te330$.

Figure 3 is the temperature dependence of the electron mobility for $Al_{0.2}Ga_{0.8}Sb-Te330$ (squares), $Al_{0.6}Ga_{0.4}Sb-Te330$ (circles), or $Al_{0.6}Ga_{0.4}Sb-Te410$ (triangles). Judging from the magnitude of the electron mobility, the band conduction of electrons is dominant in the range of the measurement temperatures. Therefore, the $n(T)$ obtained by the Hall–effect measurements is the electron concentration in the conduction band.

Figure 4 depicts $\Delta E_F(T)$ for $Al_{0.2}Ga_{0.8}Sb-Te330$ (squares), $Al_{0.6}Ga_{0.4}Sb-Te330$ (circles), and $Al_{0.6}Ga_{0.4}Sb-Te410$ (triangles), where $\Delta E_F(T)$ is calculated as[40]

$$\Delta E_F(T) = kT \ln\left[\frac{N_C(T)}{n(T)}\right]. \tag{29}$$

In this calculation, m_n^* and M_C are 0.13 and 1 for $Al_{0.2}Ga_{0.8}Sb$, while they are 0.32 and 3 for $Al_{0.6}Ga_{0.4}Sb$.[42] Although the Te-doping densities for these $Al_{0.6}Ga_{0.4}Sb$ epilayers are expected to be equal or higher than that for the $Al_{0.2}Ga_{0.8}Sb$ epilayer, the $\Delta E_F(T)$ for these $Al_{0.6}Ga_{0.4}Sb$

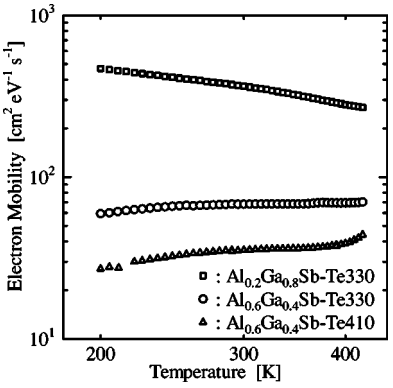

FIG. 3. Temperature dependence of electron mobility.

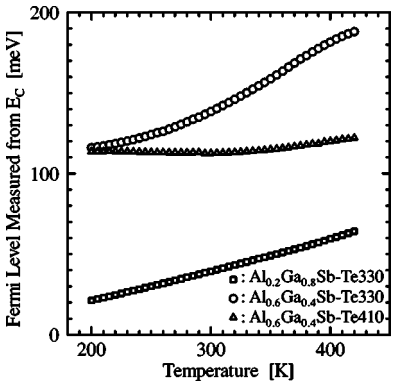

FIG. 4. Temperature dependence of Fermi level measured from E_C.

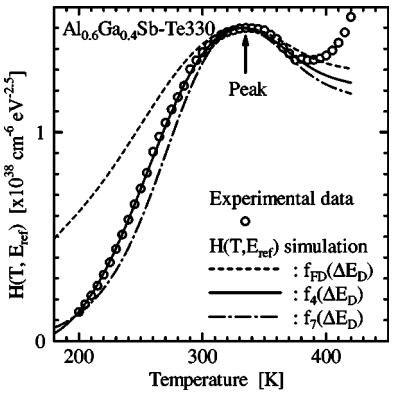

FIG. 6. The FCCS signal with $E_{\mathrm{ref}}=0.034$ eV for $Al_{0.6}Ga_{0.4}Sb-Te330$, and FCCS simulations for three kinds of distribution functions.

epilayers are much deeper than the $\Delta E_F(T)$ for the $Al_{0.2}Ga_{0.8}Sb$ epilayer.

In $Al_{0.2}Ga_{0.8}Sb-Te330$, the FCCS signal exhibits two peaks. From each peak, the energy level ΔE_{Di} and density N_{Di} of the corresponding donor species are determined. The values of ΔE_{D2} and N_{D2} are determined as 39.6 meV and 3.72×10^{17} cm^{-3}, while ΔE_{D3} and N_{D3} are 61.1 meV and 6.22×10^{16} cm^{-3}. These donor levels are similar to Te donor levels ($\sim$20 and $\sim$80 meV) in GaSb.[7] Moreover, this epilayer is found to include the shallow donors completely ionized below the lowest measurement temperature. The value of $N_{D1}-N_{A,\mathrm{total}}$ is estimated as 1.36×10^{17} cm^{-3}, where N_{D1} is the density of the shallow donors.

Figure 5 shows the experimental $n(T)$ (squares) and the $n(T)$ simulation (solid curve) using $f_{FD}(\Delta E_D)$ and Eqs. (20) and (21) with the determined values. Since the $n(T)$ simulation is in good conformity with the experimental $n(T)$, the values determined by the FCCS are considered to be reliable. In $T_{\mathrm{Te}}=330$ °C, therefore, the Te-doping density is expected to be in the order of 10^{17} cm^{-3} in our epilayers.

The circles in Fig. 6 represent the FCCS signal with $E_{\mathrm{ref}}=0.034$ eV for $Al_{0.6}Ga_{0.4}Sb-Te330$. Although the FCCS signal increases with T at $T>400$ K, this phenomenon arises from the intrinsic behavior already mentioned in Fig. 2. Since one peak appears in this figure, one type of donor species is dominant in this epilayer. Using $f_{FD}(\Delta E_D)$, the values of N_D, ΔE_D, and $N_{A,\mathrm{total}}$ are determined as 3.15×10^{17} cm^{-3}, 92.1 meV, and 1.71×10^{17} cm-3, respectively. The ratio of $N_{A,\mathrm{total}}$ to N_D is 0.54, which seems too high.

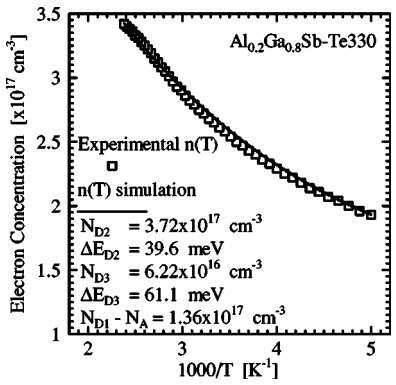

FIG. 5. Experimental and simulated $n(T)$ for $Al_{0.2}Ga_{0.8}Sb-Te330$.

In the case of $f_l(\Delta E_D)$, on the other hand, since the excited-state levels of Te donors are uncertain to date, the ΔE_r is assumed to be

$$\Delta E_r = E_1\frac{1}{r^2} \quad (r \geqslant 2) \tag{30}$$

from Eq. (18). Since the strain field around the donor can be assumed to be relaxed when the electron bound to the ground state is transferred to the excited states or the conduction band, the E_1 is tentatively considered to be 24 meV, which is calculated by Eq. (18) with $m_n^*=0.32$ and $\epsilon_s=13.5$.[43] In this case, the values of N_D, ΔE_D, and $N_{A,\mathrm{total}}$ are determined as 1.4×10^{17} cm^{-3}, 126 meV, and 2.5×10^{16} cm^{-3} for $f_4(\Delta E_D)$, respectively, while they are 1.1×10^{17} cm^{-3}, 150 meV, and 1.9×10^{14} cm^{-3} for $f_7(\Delta E_D)$, respectively. Since the Te donor density should be in the order of 10^{17} cm^{-3} according to the result in $Al_{0.2}Ga_{0.8}Sb-Te330$, the value of N_D determined using each distribution function is considered to be reasonable. On the other hand, since it is clear from the result in undoped $Al_{0.6}Ga_{0.4}Sb$ that the $N_{A,\mathrm{total}}$ should be higher than 10^{15} cm^{-3}, the value of $N_{A,\mathrm{total}}$ determined using $f_7(\Delta E_D)$ is not reasonable. Furthermore, the $N_{A,\mathrm{total}}$ determined using $f_{FD}(\Delta E_D)$ seems too high.

Using a set of N_D, ΔE_D, and $N_{A,\mathrm{total}}$ determined using each distribution function as well as $\Delta E_F(T)$ calculated with Eq. (29) by interpolating the experimental $n(T)$ with a cubic smoothing natural spline function at intervals of 0.1 K, the corresponding $H(T,E_{\mathrm{ref}})$ is simulated by

$$H(T,E_{\mathrm{ref}}) = \frac{N_D}{kT}\exp\left(-\frac{\Delta E_D - E_{\mathrm{ref}}}{kT}\right)I(\Delta E_D) - \frac{N_{A,\mathrm{total}}N_{C0}}{kT}\exp\left[\frac{E_{\mathrm{ref}}-\Delta E_F(T)}{kT}\right], \tag{31}$$

which is easily derived from Eq. (25). Figure 6 is also three $H(T,E_{\mathrm{ref}})$ simulations using $f_{FD}(\Delta E_D)$ (broken curve), $f_4(\Delta E_D)$ (solid curve), and $f_7(\Delta E_D)$ (chain curve). The solid curve is in agreement with the experimental $H(T,E_{\mathrm{ref}})$ better than the others, indicating that a set of N_D, ΔE_D, and $N_{A,\mathrm{total}}$ determined using $f_4(\Delta E_D)$ is more reliable than the others. Therefore, it is considered that the first, second, and third excited states mainly affect the $n(T)$.

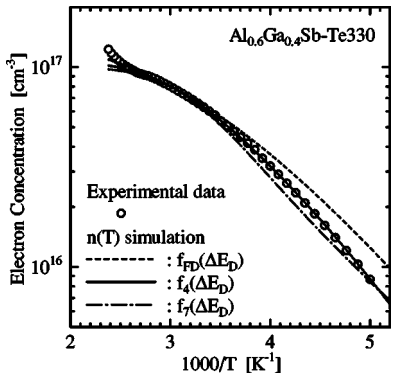

FIG. 7. The experimental $n(T)$ and three $n(T)$ simulated using values determined by the FCCS.

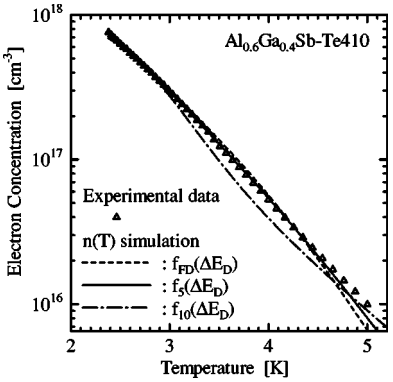

FIG. 9. The experimental $n(T)$ and three $n(T)$ simulated using values determined by the FCCS.

Figure 7 shows the experimental $n(T)$ (circles) and three $n(T)$ simulated using Eqs. (20) and (21) with the determined values. The broken, solid, and chain curves represent the $n(T)$ simulations for $f_{FD}(\Delta E_D)$, $f_4(\Delta E_D)$, and $f_7(\Delta E_D)$, respectively.[44] In the figure, the solid curve coincides with the experimental $n(T)$ more than the others, suggesting that $f_4(\Delta E_D)$ is most suitable for this epilayer.

In the above determination, only the value of E_1 is ambiguous. Using the various values of E_1, the values of N_D, ΔE_D, and $N_{A,\text{total}}$ are determined from the peak in Fig. 6, and the $H(T,E_{\text{ref}})$ simulations are also carried out. However, the $H(T,E_{\text{ref}})$ simulation is found to be almost independent of E_1, although N_D, ΔE_D, and $N_{A,\text{total}}$ are a little different. When $E_1=120$ meV, for example, the values of N_D, ΔE_D, and $N_{A,\text{total}}$ are determined as 1.4×10^{17} cm^{-3}, 131 meV, and 1.9×10^{16} cm^{-3} for $f_4(\Delta E_D)$, respectively. Although the values of N_D, ΔE_D, and $N_{A,\text{total}}$ slightly depend on E_1, therefore, they are considered to be $\sim1.4\times10^{17}$ cm^{-3}, $\sim$130 meV, and $\sim2\times10^{16}$ cm^{-3}, respectively.

The triangles in Fig. 8 represent the FCCS signal with $E_{\text{ref}}=0.172$ meV for $Al_{0.6}Ga_{0.4}Sb-Te410$. Since one peak appears in the figure, one type of donor species is dominant in this epilayer. The values of N_D, ΔE_D, and $N_{A,\text{total}}$ determined from this peak are 9.0×10^{18} cm^{-3}, 119 meV, and 2.4×10^{18} cm^{-3} for $f_{FD}(\Delta E_D)$, respectively. The value of $N_{A,\text{total}}/N_D$ is 0.27, which seems too high. On the other hand, they are 2.1×10^{18} cm^{-3}, 161 meV, and 7.7×10^{16} cm^{-3} for $f_5(\Delta E_D)$, respectively, while they are 1.7×10^{18} cm^{-3}, 173 meV, and 1.5×10^{16} cm^{-3} for $f_{10}(\Delta E_D)$, respectively, where E_1 is assumed to be 24 meV. The ΔE_D for $Al_{0.6}Ga_{0.4}Sb-Te410$ is found to be deeper than the ΔE_D for $Al_{0.6}Ga_{0.4}Sb-Te330$.

Using a set of N_D, ΔE_D, and $N_{A,\text{total}}$ determined using each distribution function as well as $\Delta E_F(T)$ calculated with Eq. (29), the $H(T,E_{\text{ref}})$ is simulated with Eq. (31) and shown by the broken, solid, and chain curves in Fig. 8 for $f_{FD}(\Delta E_D)$, $f_5(\Delta E_D)$, and $f_{10}(\Delta E_D)$, respectively. Although the broken and chain curves are in poor conformity with the experimental $n(T)$, the solid curve is in good agreement with it. Therefore, the first to fourth excited states undoubtedly affect the $n(T)$. As a result, the higher excited state influences the $n(T)$ for $Al_{0.6}Ga_{0.4}Sb-Te410$ than that for $Al_{0.6}Ga_{0.4}Sb-Te330$. This may be related to the facts that the ΔE_D for $Al_{0.6}Ga_{0.4}Sb-Te410$ is deeper than the ΔE_D for $Al_{0.6}Ga_{0.4}Sb-Te330$ and that the ΔE_F for $Al_{0.6}Ga_{0.4}Sb-Te410$ is closer to E_V than the ΔE_F for $Al_{0.6}Ga_{0.4}Sb-Te330$.

Figure 9 shows the experimental $n(T)$ (triangles) and three $n(T)$ simulated using Eqs. (20) and (21) with the determined values. The broken, solid, and chain curves represent the $n(T)$ simulations for $f_{FD}(\Delta E_D)$, $f_5(\Delta E_D)$, and $f_{10}(\Delta E_D)$, respectively. From the figure, the solid curve coincides with the experimental $n(T)$ more than the others, suggesting that $f_5(\Delta E_D)$ is suitable for the analysis of the $n(T)$ for $Al_{0.6}Ga_{0.4}Sb-Te410$.

Figure 10 depicts $g_{D5}(\Delta E_D)$ for $Al_{0.6}Ga_{0.4}Sb$. It is found

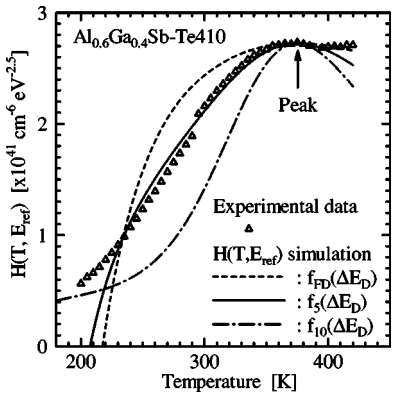

FIG. 8. The FCCS signal with $E_{\text{ref}}=0.172$ eV for $Al_{0.6}Ga_{0.4}Sb-Te410$, and FCCS simulations for three kinds of distribution functions.

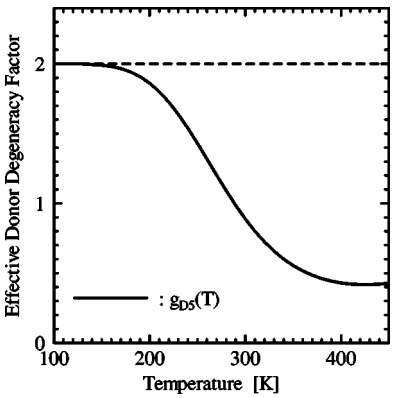

FIG. 10. Effective donor degeneracy factor for $f_5(\Delta E_D)$.

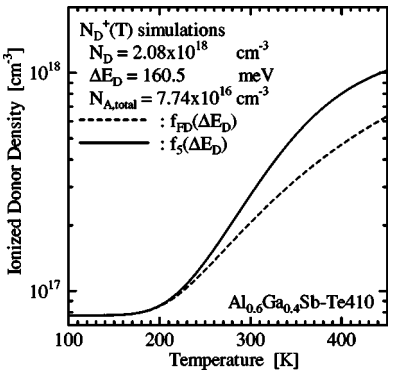

FIG. 11. Temperature dependence of ionized donor densities simulated with the same values of N_D, ΔE_D, and N_A for $f_{FD}(\Delta E_D)$ or $f_5(\Delta E_D)$.

that $g_{D5}(\Delta E_D)$ at >140 K is smaller than 2 [i.e., the donor degeneracy factor for $f_{FD}(\Delta E_D)$]. Next, we investigate how the smaller values affect the ionization efficiency of Te donors.

Figure 11 is the temperature dependence of the ionized donor density $N_D^+(T)$ simulated with the same values of N_D, ΔE_D, and $N_{A,\mathrm{total}}$ for $f_{FD}(\Delta E_D)$ (broken curve) or $f_5(\Delta E_D)$ (solid curve). Both the $N_D^+(T)$ are constant and equal to 7.74×10^{16} cm^{-3} at <140 K, because some of Te donors are positively charged due to the ionization of all the acceptors. On the other hand, the $N_D^+(T)$ for $f_5(\Delta E_D)$ is higher than the $N_D^+(T)$ for $f_{FD}(\Delta E_D)$ at elevated temperatures. For example, the $N_D^+(T)$ for $f_5(\Delta E_D)$ is higher by 1.7 than the $N_D^+(T)$ for $f_{FD}(\Delta E_D)$ at 400 K. In other words, the excited states of the Te donors enhance the ionization efficiency of the Te donors at elevated temperatures.

VI. CONCLUSION

We investigated $n(T)$ for Te-doped $Al_xGa_{1-x}Sb$ epilayers. It was found that the donor level of Te was deep in $Al_{0.6}Ga_{0.4}Sb$ while it was shallow in $Al_{0.2}Ga_{0.8}Sb$. In order to analyze the $n(T)$ for Te-doped $Al_{0.6}Ga_{0.4}Sb$, the distribution function including the influence of the excited states of donors was elucidated to be necessary. Moreover, the ionization efficiency of deep Te donors at elevated temperatures was found to be higher than expected.

ACKNOWLEDGMENTS

The authors would like to thank Professor W. Susaki and M. Segawa of Osaka Electro-Communication University for the $Al_xGa_{1-x}Sb$ sample preparation. This work was partially supported by the Academic Frontier Promotion Projects of the Ministry of Education, Culture, Sports, Science and Technology 1998-2002 and 2003-2008.

[1]G. W. Turner, H. K. Choi, and M. J. Manfra, Appl. Phys. Lett. **72**, 879 (1998).
[2]K. Y. Cheng, G. L. Pearson, R. S. Bauer, and D. J. Chandi, Bull. Am. Phys. Soc. **21**, 365 (1976).
[3]O. Madelung and M. Schulz, *Landolt-Börnstein* Vol. III/22a (Spring, Berlin, 1987), p. 139.
[4]N. Chand, T. Henderson, J. Klem, W. T. Masselink, R. Fischer, Y.-C. Chang, and H. Morkoç, Phys. Rev. B **30**, 4481 (1984).
[5]E. F. Schubert, *Doping in III-V Semiconductors* (Cambridge University Press, Cambridge, 1993), p. 355.
[6]M. Mizuta, M. Tachikawa, H. Kukimoto, and S. Minomura, Jpn. J. Appl. Phys., Part 2 **24**, L143 (1985).
[7]O. Madelung, *Semiconductors: Data Handbook*, 3rd ed. (Springer, Berlin, 2004), p. 136.
[8]D. V. Lang, J. Appl. Phys. **45**, 3023 (1974).
[9]D. K. Schroder, *Semiconductor Materials and Device Characterization*, 2nd ed. (Wiley, New York, 1998), pp. 276 and 290.
[10]H. Matsuura and K. Sonoi, Jpn. J. Appl. Phys., Part 2 **35**, L555 (1996).
[11]H. Matsuura, Jpn. J. Appl. Phys., Part 1 **36**, 3541 (1997).
[12]H. Matsuura, Y. Uchida, T. Hisamatsu, and S. Matsuda, Jpn. J. Appl. Phys., Part 1 **37**, 6034 (1998).
[13]H. Matsuura, T. Kimoto, and H. Matsunami, Jpn. J. Appl. Phys., Part 1 **38**, 4013 (1999).
[14]H. Matsuura, Y. Uchida, N. Nagai, T. Hisamatsu, T. Aburaya, and S. Matsuda, Appl. Phys. Lett. **76**, 2092 (2000).
[15]H. Matsuura, Y. Masuda, Y. Chen, and S. Nishino, Jpn. J. Appl. Phys., Part 1 **39**, 5069 (2000).
[16]H. Matsuura, K. Morita, K. Nishikawa, T. Mizukoshi, M. Segawa, and W. Susaki, Jpn. J. Appl. Phys., Part 1 **41**, 496 (2002).
[17]H. Matsuura, K. Aso, S. Kagamihara, H. Iwata, T. Ishida, and K. Nishikawa, Appl. Phys. Lett. **83**, 4981 (2003).
[18]S. Kagamihara, H. Matsuura, T. Hatakeyama, T. Watanabe, M. Kushibe, T. Shinohe, and K. Arai, J. Appl. Phys. **96**, 5601 (2004).
[19]H. Matsuura, H. Nagasawa, K. Yagi, and T. Kawahara, J. Appl. Phys. **96**, 7346 (2004).
[20]H. Matsuura, New J. Phys. **4**, 12.1 (2002) [http://www.njp.org/].
[21]H. Matsuura, Mater. Sci. Forum **389–393**, 679 (2002).
[22]H. Matsuura, K. Sugiyama, K. Nishikawa, T. Nagata, and N. Fukunaga, Mater. Sci. Forum **433–436**, 447 (2003).
[23]H. Matsuura, K. Sugiyama, K. Nishikawa, T. Nagata, and N. Fukunaga, J. Appl. Phys. **94**, 2234 (2003).
[24]H. Matsuura *et al.*, Phys. Status Solidi C **0**, 2214 (2003).
[25]H. Matsuura, J. Appl. Phys. **95**, 4213 (2004).
[26]H. Matsuura *et al.*, J. Appl. Phys. **96**, 2708 (2004).
[27]M. Ikeda, H. Matsunami, and T. Tanaka, Phys. Rev. B **22**, 2842 (1980).
[28]O. Madelung, *Semiconductors: Data Handbook*, 3rd ed. (Springer, Berlin, 2004), p. 109.
[29]A. Schöner, N. Nordell, K. Rottner, R. Helbig, and G. Pensl, Inst. Phys. Conf. Ser. **142**, 493 (1996).
[30]T. Troffer, M. Schadt, T. Frank, H. Itoh, G. Pensl, J. Heindl, H. P. Strunk, and M. Maier, Phys. Status Solidi A **162**, 277 (1997).
[31]N. Schulze, J. Gajowski, K. Semmelroth, M. Laube, and G. Pensl, Mater. Sci. Forum **353–356**, 45 (2001).
[32]G. Pensl, Mater. Sci. Forum **433–436**, 365 (2003).
[33]D. J. Kim, D. Y. Ryu, N. A. Bojarczuk, J. Karasinski, S. Guha, S. H. Lee, and J. H. Lee, J. Appl. Phys. **88**, 2564 (2000).
[34]K. F. Brennan, *The Physics of Semiconductors with Applications to Optoelectronic Devices* (Cambridge University Press, Cambridge, 1999), p. 292.
[35]P. Y. Yu and M. Cardona, *Fundamentals of Semiconductors: Physics and Materials Properties*, 2nd ed. (Springer, Berlin, 1999), p. 156.
[36]E. F. Schubert, *Doping in III-V Semiconductors* (Cambridge University Press, Cambridge, 1993), p. 13.
[37]B. Sapoval and C. Hermann, *Physics of Semiconductors* (Springer, New York, 1993), p. 73.
[38]J. Singh, *Semiconductor Devices: An Introduction* (McGraw-Hill, New York, 1994), p. 110.
[39]P. Y. Yu and M. Cardona, *Fundamentals of Semiconductors: Physics and Materials Properties*, 2nd ed. (Springer, Berlin, 1999), p. 160.
[40]S. M. Sze, *Physics of Semiconductor Devices*, 2nd ed. (Wiley, New York, 1981), pp. 17 and 23.
[41]S. M. Sze, *Modern Semiconductor Device Physics* (Wiley, New York, 1998), p. 539.
[42]Since the values of m_n^* are 0.041 and 0.50 for GaSb and AlSb, m_n^* is simply assumed to be $0.041\times(1-x)+0.50\times x$ for $Al_xGa_{1-x}Sb$.
[43]Since the values of ϵ_s are 15.7 and 12.0 for GaSb and AlSb, ϵ_s is simply assumed to be $15.7\times(1-x)+12.0\times x$ for $Al_xGa_{1-x}Sb$.
[44]The values of N_D, ΔE_D, and $N_{A,\mathrm{total}}$ determined by the curve-fitting procedure using $f_{FD}(\Delta E_D)$ are close to those determined by the FCCS using $f_{FD}(\Delta E_D)$. Therefore, the $n(T)$ simulation is similar to the broken line in Fig. 7.